NACA TN 2693 0906

TECH LIBRARY KAFB, NM
0065541

NATIONAL ADVISORY COMMITTEE FOR AERONAUTICS

TECHNICAL NOTE 2693

A THEORY AND METHOD FOR APPLYING INTERFEROMETRY TO THE MEASUREMENT OF CERTAIN TWO-DIMENSIONAL GASEOUS DENSITY FIELDS

By Walton L. Howes and Donald R. Buchele

Lewis Flight Propulsion Laboratory
Cleveland, Ohio

Washington
April 1952

AFMDC
TECHNICAL LIBRARY
AFL 2811

TECH LIBRARY KAFB, NM
0065541

TABLE OF CONTENTS

Page

SUMMARY 1

INTRODUCTION. 1

PRINCIPLES OF METHOD. 3
Light Path in Flow Field. 4
Optical Path Relation of Interfering Light Waves. 7
Optical Distortion. 11
Evaluation Equations. 12
Convergence Considerations. 15

EVALUATION PROCEDURE. 16

NUMERICAL EXAMPLE 17

SHIFT OF OBJECT PLANE 22

GENERAL DISCUSSION AND CONCLUSIONS. 24

APPENDIX A - SYMBOLS. 26

APPENDIX B - LIGHT PATH IN FLOW FIELD 29

APPENDIX C - OPTICAL PATH RELATION. 32

APPENDIX D - OPTICAL DISTORTION 36

REFERENCES. 37

2R

NATIONAL ADVISORY COMMITTEE FOR AERONAUTICS

TECHNICAL NOTE 2693

A THEORY AND METHOD FOR APPLYING INTERFEROMETRY TO THE MEASUREMENT OF CERTAIN TWO-DIMENSIONAL GASEOUS DENSITY FIELDS

2339

By Walton L. Howes and Donald R. Buchele

SUMMARY

A theory and method are described for the application of interferometry to the measurement of certain two-dimensional gaseous density fields. The theory includes the effects of optical refraction upon the observed interference pattern. Exact equations denoting the relative density difference corresponding to an observed interference-fringe shift and the optical distortion caused by refraction are derived. Corresponding approximations in the form of power series expansions are developed to permit practical application of the theory. Expressions are derived which permit calculation of the values of the power series coefficients from experimental data.

The approximations were applied to available interference data in order to determine the density distribution in a boundary layer formed by supersonic air flow along a flat plate. Good agreement was obtained between the density distribution calculated from the interference data and that obtained from pressure-probe measurements.

Various methods for verifying the theory are considered and an evaluation process is outlined.

INTRODUCTION

In investigations of high subsonic and supersonic gas flow, where compressibility of the gas necessitates the treatment of density as a variable, various optical methods (reference 1) have been utilized as a means of density measurement. This is possible because density variations in optical media such as air act in a measurable way on light. Moreover, optical methods of investigation possess the advantage of permitting instantaneous recording of the flow without disturbing the flow. Of the optical methods, quantitative investigations by the method of interferometry have proved most successful. Interferometric investigations of flow fields have been conducted primarily with interferometers of the Zehnder-Mach type. The principles of interferometry and the Zehnder-Mach interferometer have been described elsewhere (references 2 and 3).

The analysis by means of interferometry of density distributions within optical media is based on the concept of "optical path differences" of interfering light waves: the optical path is defined as the integrated product of the physical path traversed by a given wavefront and the refractive index along that path. Thus, for convenience, optical path differences will be expressed in terms of refractive index rather than density. The two quantities are related by the Lorentz-Lorenz law (reference 2). Also, for purposes of clarification, the mathematical development is conducted on the basis of the ray theory rather than the wave theory of light propagation. This is possible because light rays are functions of the light waves in that a ray indicates the direction of light propagation, which, in nonpolarizing media, is normal to an advancing wavefront. 2339

In cases such as that considered herein, where the density varies in a direction inclined to the direction of propagation of the light, the mathematical expression of optical path differences is complicated by curvature, or refraction, of the light rays.

Refraction of light in gas flow investigations by the method of interferometry has been considered by Weyl (unpublished), Bershader (reference 4), Wachtell (reference 5), Blue (reference 6), and others. An optimum wind tunnel span for minimum optical refraction error was determined by F. J. Weyl in an unpublished analysis. The first two terms (constant gradient assumption) of a Maclaurin series expansion were effectively utilized for refractive index. Optical path differences introduced outside the flow field were neglected. This derivation was applied in reference 4 to an investigation of supersonic air flow in a channel. More recently, Weyl's analysis was expanded by the inclusion of additional optical path differences arising outside the flow field and by an expansion of the Maclaurin series representation of refractive index to several terms (see reference 5). A novel method of analysis was used in reference 6 to investigate boundary layers in supersonic flow.

The present analysis attempts to include refraction effects in a practical method for evaluating two-dimensional gaseous density fields in cases where the greatest space change of density exists essentially in one direction. The analysis was carried out at the NACA Lewis laboratory. One coordinate axis of a Cartesian coordinate system is oriented parallel to the density gradient. The unknown refractive index, or density, distribution is then expressed as a Maclaurin series with respect to that coordinate. The succeeding analysis is essentially an extension and modification of the analysis of reference 5. On the basis of the succeeding analysis, a procedure for evaluating the data obtained from interferograms is described and applied to determine the density distribution in a boundary layer formed by supersonic air flow along a flat plate. Various methods are discussed for verifying the analysis.

PRINCIPLES OF METHOD

A schematic diagram of the Zehnder-Mach interferometer apparatus as used in the investigation of flow-density fields is shown in figure 1. The experimental apparatus consists of a wind tunnel having a rectangular cross section bounded on two sides by plane-parallel glass windows and a Zehnder-Mach interferometer positioned with respect to the wind tunnel so that light (from a monochromatic point source) comprising one of the divided collimated light beams is incident to the wind tunnel in a direction perpendicular to the windows. The recombined light beams are received by a camera which is focussed to image sharply some desired plane, for example, plane O_R-O_R in figure 1, within the wind tunnel and parallel to the windows. When flow is initiated, the resulting nonuniform density field is two-dimensional with all density gradients essentially perpendicular to the direction of the incident light.

2339

With the interferometer in correct adjustment and a condition of no flow existing in the wind tunnel, an interference pattern consisting of either a field of uniform brightness or a series of alternate bright and dark bands, or fringes, may be observed at the image plane corresponding to the plane I-I of figure 1. The phase of interference produced at any point of the image plane I-I by the superposition of coherent waves is determined by the optical path difference OPD of those pairs of light rays which originate at the same point of the light source and intersect at the same point in the image plane.

When flow conditions are established in the wind tunnel, the interference fringes observed at the image plane may change their position and shape. The fringe shift at each point of the image is measured with respect to some reference pattern, such as the fringe pattern obtained for no-flow conditions, or the fringe pattern representing some specific region of the flow field, for example, the free-stream region, for which the density can be determined. A specific region of the flow field is adopted as the frame of reference in the present report. A detailed diagram of the light paths is shown in figure 2. Because the observed fringe shifts are attributable to the establishment of flow conditions in the wind tunnel, the light path from the source to the initial flow-boundary is the same for both no-flow and flow conditions. Therefore, the observed fringe shifts may be regarded as a function of only that portion of the light path which is bounded by the initial flow boundary, B_I-B_I and the image plane I-I. Thus figure 2 includes only the region of interest from the initial flow boundary B_I-B_I of the wind tunnel to the image plane I-I. For convenience a ray R_2, which circumvents the wind tunnel, is shown superimposed upon the wind tunnel.

Light Path in Flow Field

In order to relate the unknown density field to the observational data secured by the method of interferometry, the mathematical relation between the density field and the observed fringe shifts must be established. This relation may be obtained by treating the evaluation of the two-dimensional field as a problem in one dimension whenever the density gradient may be treated as a function of only one Cartesian coordinate. Consider two Cartesian coordinate axes y and η both parallel to the density gradient to be investigated and lying in a plane perpendicular to the direction of the light path at the initial flow boundary B_I-B_I. (All symbols are defined in appendix A.) Let the y origin be located at a convenient point along the density gradient and at the initial boundary B_I-B_I in figures 1 and 2. Let the η origin be in the plane B_I-B_I and at that value of y at which any designated light ray $i = 0,1,2,\ldots$ enters the flow field. Let η increase positively in the direction of increasing density. Let the units of η and y be identical. Then η and y are related by the transformation 2339

$$\eta = \left|y - y_i\right| \tag{1}$$

where y_i refers to the y-ordinate value at which the light ray i enters the flow field, and

$$\left|\frac{d\eta}{dy}\right| \equiv 1 \tag{2}$$

The y-coordinate serves to locate individual light rays with respect to the unknown density field whereas use of the η-coordinate permits the mathematical expression of the ray paths in the simplest form.

In order to interpret the unknown density distribution in terms of the observed interference pattern, the paths of light rays corresponding to interfering light waves must be determined. The light path is given by Fermat's principle as that path for which the time of transit between two points in space attains a stationary value, usually a minimum. Thus

$$\int dt = \int \frac{ds}{v} = \text{stationary value} \tag{3}$$

By definition the velocity v of light propagation is related to the refractive index μ of the medium by

$$\mu = c/v \tag{4}$$

where c is the velocity of light propagation in vacuum. The differential ds of physical path length is given by

$$ds = \sqrt{1 + \left(\frac{d\eta}{dx}\right)^2}\, dx \tag{5}$$

Then equation (3) becomes

$$\int dt = \frac{1}{c}\int \mu \sqrt{1 + \left(\frac{d\eta}{dx}\right)^2}\, dx = \text{stationary value} \tag{6}$$

2339

Let quantities possessing only the subscript i, referring to a given light ray, represent values of the quantities at the initial boundary B_I-B_I of the unknown density field. Let quantities which are starred, or subscripted and starred, refer to values of the quantities at the final boundary B_F-B_F of the unknown density field. Then the solution of the variation problem (equation (6)), as obtained from Euler's equation (appendix B), is

$$1 + \left(\frac{d\eta}{dx}\right)^2 = \left(\frac{\mu}{\mu_i}\right)^2 \tag{7}$$

which satisfies the boundary conditions

$$0 \leq x \leq x^*$$

$$0 \leq \eta \leq \eta_i^*$$

$$\left(\frac{d\eta}{dx}\right)_{\eta=0} = \left(\frac{dy}{dx}\right)_{y=y_i} = 0$$

and possesses a real solution only when $\mu(\eta) \geq \mu_i$, that is, when the refractive index is a monotonic increasing function of η in which case the light ray curves, or refracts, in the xy-plane toward the direction of increased refractive index.

Outside the unknown density field, the refractive index is constant within each medium; hence, it follows from Fermat's principle that the light paths are straight lines. The external path lengths can be determined from the geometrical configuration of the experimental setup.

Equation (7) may be rewritten as the integral equation

$$\int_0^{x^*} dx = \int_0^{\eta^*} \frac{d\eta}{\sqrt{\left(\frac{\mu}{\mu_i}\right)^2 - 1}} \tag{8}$$

the solution of which depends upon the function μ. A series solution has been obtained from equation (7) by the following method (reference 5): assume that the refractive index distribution throughout that region of the flow field traversed by any given light ray may be represented by the Maclaurin series

$$\mu = \sum_{\nu=0}^{\infty} b_\nu \eta^\nu \tag{9}$$

2339

which converges to the value μ, where μ is the refractive index of the medium, η is the displacement of the light ray in the wind tunnel with respect to the y-ordinate value at which the ray enters the wind tunnel, and by definition,

$$\left| b_\nu \right| = \frac{1}{\nu!}\left|\left(\frac{d^\nu \mu}{dy^\nu}\right)_{y=y_1}\right| \tag{10}$$

Let the ray path in the unknown density field be represented by the Maclaurin series

$$\eta = \sum_{\sigma=0}^{\infty} c_\sigma x^\sigma \tag{11}$$

which is assumed to converge. Substitution of the series $\sum b_\nu \eta^\nu$ and the first derivative of the series $\sum c_\sigma x^\sigma$ in the differential equation (7) results in an expression in terms of powers of x and containing coefficients b_ν and c_σ. Following a suitable approximation, the relations of the coefficients b_ν and c_σ of like powers of x are

$$\left.\begin{aligned}
c_0 &= c_1 = c_3 = c_5 = \ldots = c_{2\sigma-1} = 0 \\
c_2 &= \frac{1}{2} b_1 \\
c_4 &= \frac{1}{12} b_1 b_2 \\
c_6 &= \frac{1}{180} \cdot b_1 b_2^2 + \frac{1}{40} b_1^2 b_3 \\
c_8 &= \frac{1}{5040} b_1 b_2^3 + \frac{3}{560} b_1^2 b_2 b_3 + \frac{1}{112} b_1^3 b_4 \\
&\ \ \vdots
\end{aligned}\right\} \tag{12}$$

where $c_0 = 0$ because $\eta = 0$ at $x = 0$. Thus, the path of a given light ray i in the field μ is given to a close approximation by

$$\eta = \frac{1}{2} b_1 x^2 + \frac{1}{12} b_1 b_2 x^4 + \left(\frac{1}{180} b_1 b_2^2 + \frac{1}{40} b_1^2 b_3\right) x^6 +$$

$$\left(\frac{1}{5040} b_1 b_2^3 + \frac{3}{560} b_1^2 b_2 b_3 + \frac{1}{112} b_1^3 b_4\right) x^8 + \ldots \tag{13}$$

2339

The location of the light ray at the final boundary B_F-B_F is found by replacing η by $\eta_i^* = |y_i^* - y_i|$ and x by x^*. Details of the derivation of equation (13) are given in appendix B.

In addition to the ray path, the angle α, through which the light ray is refracted in the unknown density field, is also of interest. By means of the substitution

$$\tan \alpha = \frac{d\eta}{dx} \tag{14}$$

in equation (7) the angle α may be expressed as

$$\cos \alpha = \frac{\mu_i}{\mu} \tag{15}$$

Optical Path Relation of Interfering Light Waves

The unknown density field and the observed interference pattern are related by the optical path difference of interfering light waves. The case of a two-dimensional density field contained in a wind tunnel is represented by figure 2. In the figure, line R_1, which intersects points A_1, A_2, A_3, A_4, and P, represents the path of any arbitrary light ray which traverses the unknown density field. Superimposed on the diagram for convenience, the line R_2 (which intersects points B_1, B_2, B_3, B_5, B_4, the focal point F on the lens L-L, and P), represents the path of a light ray which circumvents the unknown field and intersects the light ray R_1 at point P in the selected image plane I-I. Rays R_1 and R_2 are constructed parallel to the optical axis at the initial flow boundary B_I-B_I and are assumed to originate at the same point of the interferometer light source. According to the latter condition, the light waves associated with these rays are coherent and therefore may interfere.

The parallel construction of light rays R_1 and R_2 implies that the phase of interference be constant over the image plane I-I, that is,

that the interferometer by initially adjusted for obtaining an "infinite" interference fringe. However, it can be easily shown that the succeeding analysis applies without modification for any initial fringe adjustment and spacing. If an image screen is located arbitrarily at plane I-I, then interference of the waves associated with rays R_1 and R_2 may be observed at point P. A similar situation applies to all other ray pairs emitted from the same point in the light source and intersecting at plane I-I.

According to the geometrical theory of optical image formation, there exists a conjugate object point associated with each image point such as P. In the present case it is assumed that the optical layout is such that the object point associated with P is located in the vicinity of the flow field. Thus ray R_2 intersects, or at least appears to intersect, ray R_1 somewhere in the vicinity of the flow field. 2339

Suppose that the camera lens system L-L represents a perfect optical system in the sense of Gaussian optics. Then, in general, the camera lens will produce a perfect point image of a point object when the intervening object and image spaces are represented by atmosphere under standard conditions; that is, all light rays which intersect the object point and traverse the lens will intersect at the same point in the image space. If the lens system is imperfect or if a medium, such as a glass wind-tunnel window, having a refractive index which differs from that of standard atmosphere is interposed between the object and image, or if both conditions are present then an imperfect image results. The resulting image imperfections are called geometrical aberrations. For the present, the lens L-L will be regarded as perfect.

If the wind-tunnel window is neglected and the refractive index of the object and image spaces is considered to be that of standard atmosphere, there exists a conjugate object point which is intersected by every light ray which intersects P. This object point is indicated by the intersection of the backward extension of ray R_1 from point A_3 with ray R_2. The intersection is at point P_A lying in plane O_A-O_A, which represents the apparent Gaussian object plane. Similarly, all other rays which intersect at the image plane I-I also appear to intersect at plane O_A-O_A.

Now consider the interposition of a wind-tunnel window between plane O_A-O_A and the lens L-L. Assuming that the refractive index of the surrounding medium remains that of standard atmosphere, there exists a real Gaussian object plane O_R-O_R displaced from O_A-O_A by a distance $x(t)$ independent of angle $\alpha_a{}^*$. A real object located in the plane O_R-O_R will, in the sense of Gaussian optics, appear to be located at plane O_A-O_A when the object is observed through the window. The shift $x(t)$ is given by:

$$x(t) = t\left(1 - \frac{\mu_a}{\mu_w}\right) \tag{16}$$

where μ_a and μ_w are the refractive indices of atmosphere and the window, respectively.

Next consider a train of light waves generated from point P_A and assume that the refractive index throughout the object and image spaces is that of atmosphere. According to the theory of geometrical optics, the optical paths traversed by all light waves from a given object point to the conjugate image point of a perfect optical system are equal. Thus the optical lengths defined by points P_A, A_3, A_4, P and P_A, B_2, B_3, B_5, B_4, F, P are equal. Associated with the light waves are wavefronts; a wavefront is defined as the locus of points having a constant optical distance from P_A. Since the refractive index is assumed to be constant in the object space, the wavefronts about P_A are spheres. This condition follows from the definition of optical path length. Consider the wavefront centered at P_A and intersecting point A_3. It is apparent that $\mu_a\overline{P_AA_3} = \mu_a\overline{P_AB_5}$. Since the optical path lengths from P_A to P via points A_4 and B_4 are also equal, it follows that the optical path length of ray R_1 from A_3 to P equals the optical path length of ray R_2 from B_5 to P so that these latter lengths can be neglected because they contribute zero OPD. Thus the entire OPD indicated by an observed fringe shift S at point P is represented by the OPD of rays R_1 and R_2 in the space bounded by the initial flow boundary B_I-B_I and the arc $\widehat{A_3B_5}$. The OPD of rays R_1 and R_2, as indicated by a fringe shift S_a at point P, is then given by

$$S_a\lambda = \int_{\widehat{A_1A_2}} \mu\, ds - \mu_a\, \overline{B_1B_2} + \mu_w(\overline{A_2A_3} - t) - \mu_a\, \overline{B_3B_5} \tag{17}$$

where S_a, the fringe shift in wavelengths λ of light, is measured with respect to the fringe located at P when μ is replaced by μ_a. By virtue of equations (5) and (7), equation (17) may be rewritten as

$$S_a\lambda = (\mu_i - \mu_a)\, x^* + \frac{1}{\mu_i}\int_{\sigma}^{x^*} \mu^2\, dx - \mu_i x^* + \mu_w\, (\overline{A_2A_3} - t) - \mu_a\, \overline{B_3B_5} \tag{18}$$

where, in addition to the substitution of equations (5) and (7), the factor $\mu_i x^*$ has been subtracted from the first term of equation (17), added to the second term, and the terms have been rearranged. Consequently, the first term of equation (18) represents the OPD due purely to the refractive index difference obtained for an unrefracted ray

2339

which intersects the boundary B_I-B_I at A_1, that is, at the ordinate value $\eta_1 = 0$, or $y = y_1$. The second and third terms of equation (18) represent the additional OPD incurred between the tunnel boundaries B_I-B_I and B_F-B_F as a result of refraction of ray R_1, and the fourth and fifth terms indicate the OPD introduced by the wind-tunnel window and the airspace between the window and camera lens L-L, respectively, also as the result of refraction.

The refractive indices μ_a of atmosphere and μ_δ of the flow reference region, with respect to which the fringe shifts are to be measured, are constant so that a change of refractive index within the wind tunnel from that of standard atmosphere to that of the flow reference region yields a fringe shift S_δ given by 2339

$$S_\delta\lambda = (\mu_\delta - \mu_a)x^* \tag{19}$$

which corresponds to equation (18) with the exception that the refraction terms are zero. Subtraction of equation (19) from equation (18) gives

$$S_i\lambda = (\mu_i - \mu_\delta)x^* + \frac{1}{\mu_i}\int_0^{x^*} \mu^2\,dx - \mu_i x^* + \mu_w(\overline{A_2A_3} - t) - \mu_a\,\overline{B_3B_5} \tag{20}$$

where $S_i = S_a - S_\delta$ and S_i represents the observed fringe shift in wavelengths corresponding to a given light ray i and measured with respect to the fringe pattern representing the flow reference region.

Let the location of the real object plane O_R-O_R be determined with respect to the internal surface B_F-B_F of the final wind tunnel window by

$$X = Kx^* \tag{21}$$

Then it is shown in appendix C by the application of Snell's law of optical refraction and consideration of the geometrical configuration in figure 2 that the fringe shift S_i in equation (20) is given by the exact expression

$$S_i\lambda = (\mu_i-\mu_\delta)x^* + \frac{1}{\mu_i}\int_0^{x^*} \mu^2\,dx - \mu_i x^* + \mu_a Kx^*\left[\frac{\sqrt{\mu_a^2+\mu_i^2-\mu_i^{*2}}-\mu_a}{\sqrt{\mu_a^2+\mu_i^2-\mu_i^{*2}}}\right] + t\left[\mu_w\left(\frac{\mu_w - \sqrt{\mu_w^2+\mu_i^2-\mu_i^{*2}}}{\sqrt{\mu_w^2+\mu_i^2-\mu_i^{*2}}}\right) + \frac{\mu_a^2}{\mu_w}\left(\frac{\sqrt{\mu_a^2+\mu_i^2-\mu_i^{*2}}-\mu_a}{\sqrt{\mu_a^2+\mu_i^2-\mu_i^{*2}}}\right)\right] \tag{22}$$

when the camera lens system is assumed to be perfect. For application to practical problems, equation (22) may be simplified by making suitable approximations, as shown in appendix C, with the result

$$S_i\lambda = (\mu_i - \mu_\delta)x^* + \frac{1}{\mu_i}\int_0^{x^*} \mu^2\, dx - \mu_i x^* - Kx^*(\mu_i^* - \mu_i) \tag{23}$$

Equation (23) is independent of the wind-tunnel windows, their effect upon the observed fringe shift S_i thus being negligible. Assuming that the series expansions in equations (9) and (11) are convergent, it is also shown in appendix C that their substitution in equation (23) yields

$$\mu_i - \mu_\delta = S_i \frac{\lambda}{x^*} - 2\sum_{\nu=1}^{\infty}\sum_{\sigma=2,4,6\ldots}^{\infty} \frac{b_\nu c_{\sigma\nu}}{\sigma+1} x^{*\sigma} + K\sum_{\nu=1}^{\infty}\sum_{\sigma=2,4,6\ldots}^{\infty} b_\nu c_{\sigma\nu} x^{*\sigma} \tag{24}$$

where the coefficients $c_{\sigma\nu}$ may be expressed in terms of the coefficients c_σ by equating the coefficients of like powers of x in the expression

$$\sum_{\sigma=2,4,6,\ldots}^{\infty} c_{\sigma\nu}\, x^\sigma = \left(\sum_{\sigma=2,4,6,\ldots}^{\infty} c_\sigma x^\sigma\right)^\nu \tag{25}$$

Optical Distortion

The refractive index difference $\mu_i - \mu_\delta$ given by equation (24) is associated with a given light ray i which enters the flow field at the ordinate value y_i. However, the fringe shift S_i corresponding to the ray i may appear to exist at some ordinate value $y_i + (\Delta y)_i$ other than y_i; that is, there may exist a form of optical distortion caused by refraction of the light rays in the flow field. For example, in figure 2 the light rays R_1 and R_2 appear to originate at the apparent object point P_A, whereas the refractive index μ_i, indicated by the fringe shift S_i by virtue of equation (24), exists at the y-ordinate value containing the point A_1 at which ray R_1 enters the flow field. Let the difference between the y-ordinate values containing points P_A and A_1 be termed the "optical distortion in the object space", denoted by Δy. Then, with respect to rays R_1 and R_2, the distortion may be represented after consideration of figure 2 by

$$(\Delta y)_i = \overline{A_3B_3} - (\overline{A_3B_3} + \overline{B_1A_1}) \tag{26}$$

or

$$(\Delta y)_i = \left[Kx^* - x(t) + t\right] \tan \alpha_a^* - \left[\eta_i^* + y(\alpha_w^*, t)\right] \tag{27}$$

By use of Snell's law and equations (15) and (16) it is demonstrated in appendix D that equation (27) can be presented in an exact form analogous to that of equation (22) as 2339

$$(\Delta y)_i = \left(Kx^* + \frac{\mu_a}{\mu_w} t\right)\sqrt{\frac{\mu_i^{*2} - \mu_i^2}{\mu_a^2 + \mu_i^2 - \mu_i^{*2}}} - \left(\eta_i^* + t\sqrt{\frac{\mu_i^{*2} - \mu_i^2}{\mu_w^2 + \mu_i^2 - \mu_i^{*2}}}\right) \tag{28}$$

When suitable approximations are applied, equation (28) can be rewritten to a close approximation as

$$(\Delta y)_i = Kx^* \sqrt{\mu_i^{*2} - \mu_i^2} - \eta_i^* \tag{29}$$

which like equation (23) is independent of the wind-tunnel windows. By virtue of the differential equation (7) of the ray path, the square-root term of equation (29) may be replaced by $\left(\frac{d\eta}{dx}\right)_{\eta=\eta_i}$, where $\mu_i \approx 1$, thus yielding

$$(\Delta y)_i = Kx^* \left(\frac{d\eta}{dx}\right)_{\eta=\eta_i^*} - \eta_i^* \tag{30}$$

Then η_i^* is replaced by $\sum c_\sigma x^\sigma$ and $\left(\frac{d\eta}{dx}\right)_{\eta=\eta_i^*}$, by the first derivative of $\sum c_\sigma x^\sigma$ (assuming convergence); equation (30) is now expressed in its final form

$$(\Delta y)_i = \sum_{\sigma=2,4,6,\ldots}^{\infty} (K\sigma - 1)\, c_\sigma x^{*\sigma} \tag{31}$$

Evaluation Equations

Equations (24) and (31) relate observable responses of individual light rays to the refractive index distribution in the flow field.

2339

Equation (24) may be readily transformed into an expression for the relative density change existing at the value y_i at which a given light ray i enters the flow field by applying the Gladstone-Dale approximation

$$\mu = 1 + k\rho \tag{32}$$

of the Lorentz-Lorenz law, where ρ is the gas density corresponding to the refractive index μ, and k is a constant. Thus, by substitution, equation (24) becomes

$$\frac{\rho_i - \rho_\delta}{\rho_\delta} = \frac{1}{k\rho_\delta}\left[S_i \frac{\lambda}{x^*} - 2\sum_{\nu=1}^{\infty}\sum_{\sigma=2,4,6,\ldots}^{\infty} \frac{b_\nu c_{\sigma\nu}}{\sigma + 1} x^{*\sigma} + K\sum_{\nu=1}^{\infty}\sum_{\sigma=2,4,6,\ldots}^{\infty} b_\nu c_{\sigma\nu} x^{*\sigma}\right] \tag{33}$$

which may be evaluated if the coefficients b_ν are determined.

Because of refraction of the light rays traversing the flow field, the observed interference pattern is, in general, a distorted representation of the density distribution within the field; the distortion of the fringe pattern corresponding to any given light ray being given by equation (31). In order to determine the true density field, the distortion effect must be eliminated or at least minimized in some manner.

In order to evaluate equations (33) and (31), the values of the coefficients b_ν, c_σ, and $c_{\sigma\nu}$ must be determined for each ordinate value y_i at which any given light ray i enters the flow field. Actually, if the values of the coefficients b_ν are determined, the corresponding values of the coefficients c_σ and $c_{\sigma\nu}$ are given automatically because the coefficients c_σ and $c_{\sigma\nu}$ are functions of b_ν according to equations (12) and (25), respectively. The coefficients b_ν may be evaluated if they are expressed as functions of the derivatives of the observed interference-fringe shifts with respect to y. For any given light ray i, successive differentiations of the assumed refractive-index-distribution equation (9) yields equation (10), where derivatives of the coefficients b_ν are zero because the coefficients b_ν are constant for any given light ray. Consider equation (24), which characterizes any given light ray i, where μ_i and b_ν possess fixed values. With respect to the entire manifold of rays comprising the light beam, μ and b_ν (hence $c_{\sigma\nu}$) are variables. Thus equation (24) may be rewritten without subscripts i as

$$\mu-\mu_\delta = S\,\frac{\lambda}{x^*} - 2\sum_{\nu=1}^{\infty}\sum_{\sigma=2,4,6,\ldots}^{\infty}\frac{b_\nu c_{\sigma\nu}}{\sigma+1}\,x^{*\sigma} + K\sum_{\nu=1}^{\infty}\sum_{\sigma=2,4,6,\ldots}^{\infty} b_\nu c_{\sigma\nu} x^{*\sigma} \tag{34}$$

Differentiation of equation (34) ν times with respect to y yields

$$\frac{d^\nu\mu}{dy^\nu} = \frac{\lambda}{x^*}\frac{d^\nu S}{dy^\nu} - \frac{d^\nu}{dy^\nu}\left(2\sum_{\nu=1}^{\infty}\sum_{\sigma=2,4,6,\ldots}^{\infty}\frac{b_\nu c_{\sigma\nu}}{\sigma+1}\,x^{*\sigma} - K\sum_{\nu=1}^{\infty}\sum_{\sigma=2,4,6,\ldots}^{\infty} b_\nu c_{\sigma\nu} x^{*\sigma}\right) \tag{35}$$

2339

Subsequently, it follows from equation (10) that, at any given ordinate-value y_i,

$$\left|b_\nu\right| = \frac{1}{\nu!}\left|\left\{\frac{\lambda}{x^*}\left(\frac{d^\nu S}{dy^\nu}\right)_{y=y_i} - \frac{d^\nu}{dy^\nu}\left(2\sum_{\nu=1}^{\infty}\sum_{\sigma=2,4,6,\ldots}^{\infty}\frac{b_\nu c_{\sigma\nu}}{\sigma+1}\,x^{*\sigma} - K\sum_{\nu=1}^{\infty}\sum_{\sigma=2,4,6,\ldots}^{\infty} b_\nu c_{\sigma\nu} x^{*\sigma}\right)\right\}\right| \tag{36}$$

For simplification, assume that all terms on the right-hand side of equation (36) are small compared with the first term. Then at any given ordinate value $y=y_i$

$$\left|b_\nu\right| = \frac{1}{\nu!}\,\frac{\lambda}{x^*}\left|\left(\frac{d^\nu S}{dy^\nu}\right)_{y=y_i}\right| \tag{37}$$

In cases where the preceding assumption is invalid, the effect of the neglected terms can be accounted for by the application of an iteration process, where the first approximation of b_ν is given by equation (37).

It is evident that the derivatives $\frac{d^\nu S}{dy^\nu}$ are determinable from the observed interference pattern. However, it is important to note that the true values of $\frac{d^\nu S}{dy^\nu}$, hence the desired values of b_ν, are obtained only when the distortion Δy is effectively zero throughout the region of interest. However, it follows from consideration of equation (31), that, in general, no single object plane of focus exists for which $\Delta y = 0$ for all light rays. If the ray path series $\sum c_\sigma x^\sigma$ is convergent, then the first nonzero term - for which $\sigma = 2$ - may generally

be expected to be the term of largest absolute magnitude. In the case of equation (31) this term may be reduced to zero by selecting $K = 0.5$, that is, by selecting the object plane of focus to be the midspan plane of the wind tunnel. Then equation (31) becomes

$$(\Delta y)_1 = \sum_{\sigma=4,6,8,\ldots}^{\infty} \frac{\sigma-2}{2} c_\sigma x^{*\sigma} \tag{38}$$

2339

Assuming convergence, the magnitude of equation (38) will usually be small enough so that the shape of the curve $S(y)$ will not be changed appreciably. Thus the values of the derivatives $\frac{d^\nu S}{dy^\nu}$ used to compute the values of the coefficients b_ν will be essentially unchanged by the residual distortion. If the curve $S(y)$ were changed appreciably by consideration of equation (38), then an iteration process utilizing equations (37), (36), and (38) could be performed until the desired values of b_ν and the desired curve $S(y)$ were obtained such that b_ν satisfied equation (36) and $\Delta y \rightarrow 0$ throughout the interval $0 \leqq y \leqq y_\delta$.

For $K = 0.5$, expression (33) becomes

$$\frac{\rho_1-\rho_\delta}{\rho_\delta}$$

$$= \frac{1}{k\rho_\delta}\left(S_1 \frac{\lambda}{x^*} - 2\sum_{\nu=1}^{\infty}\sum_{\sigma=2,4,6,\ldots}^{\infty} \frac{b_\nu c_{\sigma\nu}}{\sigma+1} x^{*\sigma} + \frac{1}{2}\sum_{\nu=1}^{\infty}\sum_{\sigma=2,4,6,\ldots}^{\infty} b_\nu c_{\sigma\nu} x^{*\sigma}\right) \tag{39}$$

Equations (37), (12), (25), (39), (38), and possibly (36) are sufficient for evaluating an unknown gaseous density field satisfying the restrictions imposed in the derivation.

Convergence Considerations

It is impractical to investigate convergence of the series expansions and iteration processes analytically because the exact analytic expressions for Δy and $\frac{\rho-\rho_\delta}{\rho_\delta}$ are unknown. The validity of the analysis can be indicated by comparing the results obtained by the interference method with the results obtained from other methods of analysis. For example, the resultant distribution obtained by the interference

method can be compared with that given by the theory for the density field or by some other valid experimental method. Agreement of the series solution with the other methods of solution would indicate that the series are either uniformly convergent or asymptotic representations of the unknown quantities. It is possible that the series might be asymptotic, although divergent, because the Maclaurin series possesses the form of an asymptotic series (reference 7). 2339

If the series (equations (38) and (39)) are convergent or asymptotic, then in computations utilizing these series the remainder in each case is less in absolute value than the first series term which is neglected. Thus the number of applicable terms of either series will include all successive terms for which the coefficients can be calculated with a reasonable degree of accuracy up to, but not including, the term of minimum absolute magnitude.

EVALUATION PROCEDURE

Assume that the interferometer and wind tunnel are in operational adjustment and that the interference fringes are obtainable for any desired object plane for which the interferometer camera may be focused (before flow is initiated in the wind tunnel) by observing at plane I-I (in fig. 2) the image formed by light reflected from an object inserted into the field of view at the desired object plane of focus, usually the midspan plane of the wind tunnel, for which $K = 0.5$. After the camera is focussed, the object is removed, flow is initiated, and the interferograms are obtained by means of photographic processes.

An interferogram may be evaluated according to any one of several schemes depending upon the initial choice of fringe orientation and spacing. The result of the interferogram evaluation process is an expression for the fringe shift S as a function of y for the particular experimental conditions. These values of $S(y)$ can be used in the following manner to determine the density field:

1. From the experimentally determined values of $S(y)$, obtained when $K = 0.5$, determine the values of successive derivatives $\frac{dS}{dy}$, $\frac{d^2S}{dy^2}, \ldots, \frac{d^\nu S}{dy^\nu}$ throughout the interval $0 \leq y \leq y_\delta$. These values may be determined by any one of several methods; for example, $S(y)$ may be plotted graphically. Then at any ordinate value $y=y_i$, $\left(\frac{dS}{dy}\right)_{y=y_i}$ represents the slope of the curve $S(y)$. The derivatives $\left(\frac{dS}{dy}\right)_{y=y_i}$ can be plotted. From the curve $\frac{dS(y)}{dy}$, values of $\left(\frac{d^2S}{dy^2}\right)_{y=y_i}$ for various values

$y=y_i$ can be determined as before. The process may be repeated to determine successive derivatives $\frac{d^\nu S(y)}{dy^\nu}$.

Alternatively, $S(y)$ may be represented by a polynomial $S = P_\nu(y)$. The values of successive derivatives $\left(\frac{d^\nu S}{dy^\nu}\right)_{y=y_i}$ at various ordinate values $y=y_i$ may then be calculated by taking successive derivatives of $P_\nu(y)$ with respect to y and then inserting the values $y=y_i$.

2339

2. Calculate values of the coefficients b_ν for each light ray from the values of $\left(\frac{d^\nu S}{dy^\nu}\right)_{y=y_i}$ and equation (37).

3. Determine from the preceding results $b_\nu(y)$ the magnitude of the expression which is contained in equation (36) but which is neglected in equation (37). (The coefficients $c_{\sigma\nu}$ are given by equation (25)). Calculate the residual distortion given by equation (38), where the coefficients c_σ are functions of the coefficients b_ν by virtue of equations (12). If the magnitude of the expression neglected in equation (37) is of the order of magnitude of the right-hand side of equation (37), or if correction of the residual distortion of the curve $S(y)$ results in an appreciable modification of the values of the quantities $\left(\frac{d^\nu S}{dy^\nu}\right)_{y=y_i}$ or if both these conditions are true, then the iteration processes mentioned in the section Evaluation Equations may possibly be applied to determine more accurate values of $(\Delta y)_i$ and b_ν.

4. Calculate the relative density difference $\frac{\rho_i-\rho_\delta}{\rho_\delta}$ given by equation (39) for various ordinate values $y=y_i$.

5. Plot $\frac{\rho-\rho_\delta}{\rho_\delta}$ against y, where the observed values y_i are replaced by the distortion-corrected values $y_i + (\Delta y)_i$. The resulting curve represents the desired density profile.

NUMERICAL EXAMPLE

In order to illustrate the application of the equations and procedure and to investigate attendant conditions, consider the evaluation of the density distribution along the density gradient within a boundary layer due to supersonic air flow along a flat plate.

The particular setup investigated (reference 6) consisted of a flat plate of 3.6-inch width contained in a wind tunnel of 3.6-inch span bounded by 0.5-inch-thick glass windows having a refractive index of 1.52. The interferometer light source consisted of a high-pressure mercury arc in conjunction with an interference-type filter which transmitted the green spectral line of wavelength 5461 Angstroms (2.15×10^{-5} in.). The interferometer camera was focussed to image the midspan plane of the wind tunnel.

Supersonic air flow having a free-stream Mach number of 2.0 at a density of 6.77×10^{-4} slugs per cubic foot was established. The following data were obtained from an interferogram of the boundary layer 2.5 inches downstream of the leading edge of the flat plate: 2339

Fringe Shift, S	0	-.50	-1.00	-1.50	-2.00
Distance from plate, y, inches	0.0429	0.0198	0.0165	0.0142	0.0120
S	-2.50	-3.00	-3.50	-4.00	-4.50
y, inches	0.0100	0.0083	0.0066	0.0046	0.0028

These data are presented graphically in figure 3. The first two derivatives $\frac{dS}{dy}$ and $\frac{d^2S}{dy^2}$ were determined with a tangentiometer. The resulting curves $\frac{dS(y)}{dy}$ and $\frac{d^2S(y)}{dy^2}$ are plotted in figures 4 and 5, respectively. The quantitative determination of succeeding derivatives was of questionable value. The residual distortion (indicated by equation (38)), the inherent error of the original data curve, and the error introduced by the measuring instrument would generally tend to introduce large relative errors in the measured values of succeeding derivatives.

The measured values of $\frac{dS}{dy}$ and $\frac{d^2S}{dy^2}$ and expression (37) were utilized to calculate the coefficients b_1 and b_2 for various values of y to obtain the curves $b_1(y)$ and $b_2(y)$, which are also plotted in figures 4 and 5, respectively.

With respect to the evaluation equations, if refraction of the light rays in the flow field is neglected, then series (9) and (11) reduce to $\mu = b_0$ and $\eta = 0$, respectively, and the evaluation equations (38) and (39) become, respectively,

$$(\Delta y)_i = 0 \tag{42}$$

and

$$\frac{\rho_i-\rho_\delta}{\rho_\delta} = S_i \frac{\lambda}{k\rho_\delta x^*} \tag{43}$$

which represent first approximations of the residual distortion and relative density difference. These equations have been utilized by several investigators with considerable success, especially when the optical refraction was small. Equations (42) and (43) were used to determine a first approximation of the density distribution indicated by the data of the present example. The resultant distribution is shown in figure 6. Then, by means of equations (37), (12), (25), (38), and (39) and the derivatives $\frac{dS}{dy}$ and $\frac{d^2S}{dy^2}$, the density distribution was calculated to a third approximation. The appropriate approximations were determined as follows:

From equation (37) it follows that

$$b_1 = \frac{\lambda}{x^*}\left(\frac{dS}{dy}\right)_{y=y_i} \tag{44a}$$

$$b_2 = \frac{1}{2}\frac{\lambda}{x^*}\left(\frac{d^2S}{dy^2}\right)_{y=y_i} \tag{44b}$$

By virtue of equation (12), equation (38) becomes

$$(\Delta y)_i = \frac{1}{12} b_1 b_2 x^{*4} \tag{45}$$

where only terms possessing coefficients b_ν, $\nu \leq 2$, hence c_σ, $\sigma \leq 4$, are included because only the values of derivatives $\frac{d^\nu S}{dy^\nu}$, $\nu \leq 2$, were determined. On this basis, the expansion of equation (39) is

$$\frac{\rho_i-\rho_\delta}{\rho_\delta} = \frac{1}{k\rho_\delta}\left[S_i \frac{\lambda}{x^*} - \frac{1}{6}(b_1c_{21} + b_2c_{22})x^{*2} + \frac{1}{10}(b_1c_{41} + b_2c_{42})x^{*4}\right]$$

However, by virtue of equation (25)

$$c_{21}x^{*2} + c_{41}x^{*4} = c_2x^{*2} + c_4x^{*4}$$

and

$$c_{22}x^{*2} + c_{42}x^{*4} = (c_2x^{*2} + \ldots)^2$$

so that

$$c_{21} = c_2 \qquad c_{41} = c_4 \qquad c_{22} = 0 \qquad c_{42} = c_2^2$$

Therefore, considering equation (12), the relative density difference is given by

$$\frac{\rho_i - \rho_\delta}{\rho_\delta} = \frac{1}{k\rho_\delta}\left(S_i \frac{\lambda}{x^*} - \frac{1}{12} b_1^2 x^{*2} + \frac{1}{30} b_1^2 b_2 x^{*4}\right) \tag{46}$$

2339

in the present instance.

The resultant density distribution (third approximation) indicated by equations (44a), (44b), (45), and (46) is shown in figure 6 for comparison with the first approximation. The second approximation is not shown in figure 6 because the resulting curve is nearly identical to that given by the third approximation. In addition, the third approximation of the density profile is depicted in figure 7 for comparison with the theoretical profile shown in reference 6 and the experimental profile calculated in reference 6 from total pressure measurements.

The remainders of equations (45) and (46) were obtained by expanding equations (38) and (39), respectively, to include terms containing x^{*6}, with the result

$$R_{\Delta y} = \left(\frac{1}{90} b_1^2 b_2 + \frac{1}{20} b_1^2 b_3\right) x^{*6} \tag{47}$$

and

$$R\,\frac{\rho - \rho_\delta}{\rho_\delta} = \frac{1}{k\rho_\delta}\left(\frac{2}{105} b_1^2 b_2^2 + \frac{9}{280} b_1^3 b_3\right) x^{*6} \tag{48}$$

Considering figure 5, the maximum absolute value of b_3 was found to be about 5 inches^{-3}. Thus the maximum absolute values of the remainders were found to be $\left|R_{\Delta y}\right| < 0.0001$ inch and $\left|R\,\frac{\rho - \rho_\delta}{\rho_\delta}\right| < 0.01$.

In the preceding example, the appropriate evaluation equations were developed for the case where derivatives of S of order higher than the second are neglected. As noted previously, the calculation of values of succeeding derivatives would be impractical in most cases. Thus the applicable formulas correspond to polynomials possessing coefficients

defined at the initial boundary value $x = 0$, $y = y_i$. The evaluation procedure corresponds to that which was previously described with the exception that the former equations are replaced by the expressions developed in the preceding section; that is, the coefficients b_ν are given by equations (44a) and (44b), the residual distortion is given by equation (45), and the density difference at each ordinate value y_i is calculated from equation (46).

2339

In the preceding example, the principal basis for verification of the validity of the present analysis was afforded by comparison of the density field indicated by the interferogram with that indicated by theory and by total pressure measurements. The generally good agreement of the theoretical and probe results with the interferometer result would tend to indicate that the interferogram analysis is valid and probably indicates to a good approximation the true density distribution in the present instance.

The maximum indicated density correction due to light refraction amounted to a 4-percent increase in the density difference with respect to free stream, or about 9 percent of the total density difference across the boundary layer, as depicted in figure 6. The maximum correction occurred nearest the surface of the flat plate. This correction resulted in considerably better over-all agreement between the density field indicated by the interferogram and that indicated by theory and by pressure measurements.

The maximum residual distortion was found from equation (45) to be 0.0015 inch at a distance $y = 0.015$ inch from the surface of the flat plate. The maximum absolute remainders due to termination of the series were less than 0.0001 inch distortion and 1-percent density change.

In the present example, the previously mentioned iteration processes were neglected in the determination of the coefficients b_ν and the distortion Δy. The maximum relative error of the coefficients b_ν resulting from neglect of these processes was estimated by means of a rough calculation to be about 10 or 20 percent.

The present analysis assumes that the flow field is perfectly two dimensional with the density gradient inclined essentially in one direction. This condition is, however, only approximated in practice because, for example, in the illustrative example considered herein, "end" effects (reference 4) serve to violate the assumed flow conditions. Boundary layers are formed along the surfaces of the wind-tunnel windows and adjacent to the windows and the flat plate. In the example, the effects of these deviations from the assumed conditions were assumed to be small. However, preliminary considerations indicate that "end" effect corrections would result in better agreement of the profile indicated by interference measurements with that indicated by theory and by total pressure measurements, especially in the region adjacent to the free stream.

Because no lens system is absolutely perfect it is to be expected that aberrations of the camera lens will introduce additional optical path differences and distortion (reference 8) especially when the magnitude of the optical refraction in the flow field is large and the wind tunnel-to-camera lens distance is also great. This effect is minimized by the use of a camera lens which introduces the minimum possible geometrical aberration. In the analysis and in the example, the optical path and distortion effects introduced by the camera lens were regarded as negligible.

2339

SHIFT OF OBJECT PLANE

Additional evidence of the validity of the present analysis in any given situation may be obtained by comparing the interference pattern observed at an object plane other than that denoted by $K = 0.5$ with that predicted by theory. The shift of object plane introduces a double effect upon the observed interference pattern: the phase of interference and the observed position of the interference attributed to a given light ray are shifted because both are functions of K by virtue of equations (24) and (31), respectively. The fringe shift incurred in translating the object plane from the midspan plane, corresponding to $K = 0.5$, to another plane corresponding to $K = K_1$ may be obtained from the differential of equation (24); that is,

$$dS_i = -\frac{1}{\lambda}\sum_{\nu=1}^{\infty}\sum_{\sigma=2,4,6,\ldots}^{\infty} b_\nu c_{\sigma\nu} x^{*\sigma+1}\, dK \tag{49}$$

Similarly, the change of distortion is obtained from the differential of equation (31); that is,

$$d(\Delta y)_i = \sum_{\sigma=2,4,6,\ldots}^{\infty} \sigma c_\sigma x^{*\sigma}\, dK \tag{50}$$

The shifts ΔS_i and $\Delta(\Delta y)_i$ due to a shift ΔK of the object plane are determined by integrating equations (49) and (50) between the appropriate limits. Thus, for a shift of object plane from $K = 0.5$ to $K = K_1$, ΔS_i and $\Delta(\Delta y)_i$ are given, respectively, by

$$\Delta S_i = -\frac{1}{\lambda}\left(K_1 - \frac{1}{2}\right)\sum_{\nu=1}^{\infty}\sum_{\sigma=2,4,6,\ldots}^{\infty} b_\nu c_{\sigma\nu} x^{*\,\sigma+1} \tag{51}$$

and

$$\Delta(\Delta y)_i = (K_1 - \frac{1}{2})\sum_{\sigma=2,4,6,\ldots}^{\infty} \sigma c_\sigma x^{*\sigma} \tag{52}$$

Agreement of the predicted curve $S(y)$ at $K = K_1$ obtained by means of equations (51) and (52) with the experimental result $S(y)$ would be further justification of the analysis by means of series. It is to be noted that in the case where refraction of the light rays in the flow field is neglected, no change in the interference pattern is predicted when the object plane is shifted. This condition is apparent from equations (42) and (43). Also, it is to be noted that the prediction process is not reversible; that is, the interference pattern corresponding to the object plane for which $K = 0.5$ cannot be readily determined from the interference pattern corresponding to the object plane for which $K = K_1$. This situation occurs because true values of b_ν and c_σ can be determined to a close approximation only when $\Delta y = 0$, in which case the plane for which $K = 0.5$ generally represents the optimum choice of object plane.

2339

A second set of data $S(y)$ was available for the object plane corresponding to $K = 1$, that is, the flow-boundary plane B_I-B_I nearest the light source. By means of the values of $S(y)$ for $K = 0.5$ and equations (51) and (52), the predicted curve $S(y)$ for $K = 1$ was calculated, where, as previously, only terms possessing coefficients b_ν, $\nu \leq 2$, hence c_σ, $\sigma \leq 4$, were included because only the values of derivatives $\frac{d^\nu S}{dy^\nu}$, $\nu \leq 2$, were determined. Thus the appropriate expressions are

$$\Delta S_i = -\frac{1}{4\lambda}\left(b_1^2 x^{*3} + \frac{2}{3} b_1^2 b_2 x^{*5}\right) \tag{53}$$

and

$$\Delta(\Delta y)_i = \frac{1}{2} b_1 x^{*2} + \frac{1}{6} b_1 b_2 x^{*4} \tag{54}$$

with the respective remainders

$$R_{\Delta S} = -\frac{x^{*7}}{4\lambda}\left(\frac{8}{45} b_1^2 b_2^2 + \frac{3}{10} b_1^3 b_3\right) \tag{55}$$

and

$$R_{\Delta(\Delta y)} = \frac{x^{*6}}{20}\left(\frac{1}{3} b_1^2 b_2 + \frac{3}{2} b_1^2 b_3\right) \tag{56}$$

The maximum absolute values of the remainders were found to be

$$\left|R_{\Delta S}\right| < 10^{-1} \quad \text{and} \quad \left|R_{\Delta(\Delta y)}\right| < 10^{-5} \text{ inch.}$$

The resulting curve $S(y)$ for $K = 1$ predicted by the present theory is depicted in figure 8 for comparison with the curve obtained from experimental measurements. Although the agreement of the two curves is not perfect, it is still considerably better than that obtained when refraction was neglected, as is evident from figure 8. Apparently the disagreement between the experimental result and that predicted by the present theory is caused principally by the fact that the errors of the calculated values of the coefficients b_ν were relatively large when the approximation (equation (37)) of equation (36) was used alone. Thus, because the coefficients b_ν, $\nu > 0$, comprise the major factors of equations (51) and (52), the relative errors of the quantities ΔS_i and $\Delta(\Delta y_i)$ were also large. In the case of the evaluation equation (39), the effect of errors of the calculated values of the coefficients b_ν appears only in correction terms which are small relative to the primary term. Of lesser importance is the fact that the values of the derivatives $\frac{d^\nu S}{dy^\nu}$ were determined from a curve $S(y)$ which possessed residual distortion. Thus, the measured values of the derivatives would have been in error wherever the slope of the experimental curve $S(y)$ deviated to any great extent from the slope of the desired distortion-free curve. 2339

It is concluded that the improved agreement of the predicted curve $S(y)$ for $K = 1$ (when refraction of the light rays in the flow field is considered) with the experimental curve is further evidence of the validity of the series analysis, at least for the present example.

GENERAL DISCUSSION AND CONCLUSIONS

The present analysis represents an extension and modification of Wachtell's analysis with the inclusion of a procedure for analyzing certain two-dimensional gaseous density fields by means of optical interference.

The equation of the light path in the unknown density field was developed as a power series, the coefficients of which are functions of the coefficients of a Maclaurin series representation of refractive index. An exact optical path difference equation was derived, which, when re-expressed in the form of an approximation, permitted the determination of the unknown density distribution from observed interference fringe shifts. A form of optical distortion resulting from refraction of the light rays in the unknown density field was considered. The

distortion was expressed by an exact equation and a power series. The power series was utilized to determine an object plane of focus for which the distortion is minimized and to calculate the residual distortion. Differentiation of the optical-path-difference equation permitted direct calculation of values of the first few refractive index series coefficients.

In addition, a procedure for applying the present theory was discussed and applied to determine the density distribution in a boundary layer formed by supersonic air flow along a flat plate. The resultant distribution agreed reasonably well with that given by theory and by pressure-probe measurements. Further confirmation of the theory was obtained by predicting relatively successfully the interference pattern produced for an object plane other than the optimum plane.

2339

It is concluded that the present analysis will permit increased accuracy in the determination of certain two-dimensional gaseous density distributions by the method of optical interference.

Lewis Flight Propulsion Laboratory
National Advisory Committee for Aeronautics
Cleveland, Ohio, January 3, 1952

APPENDIX A

SYMBOLS

The following symbols are used in this report:

A_1,A_2,A_3,A_4	points intersected by light ray which traverses flow field
B_F-B_F	final flow boundary traversed by light ray
B_I-B_I	initial flow boundary traversed by light ray
B_ν	binomial coefficients
B_1,B_2,B_3,B_4,B_5	points intersected by light ray which circumvents flow
b_ν	refractive index coefficient
c	velocity of light in vacuum
c_σ	light path coefficient
F	focal point of camera lens; function
I-I	image plane
K	fraction of wind tunnel span
k	constant (0.1166 ft^3/slug for air when $\lambda = 5461A$)
L-L	camera lens
O_A-O_A	apparent object plane
O_R-O_R	real object plane
OPD	optical path difference
P	image point
P_A	apparent object point
P(y)	polynomial
R	remainder

2339

2339

R_1,R_2	light rays
S	interference-fringe shift (wavelengths of light)
s	distance measured along path of light ray
t	wind-tunnel window thickness; time
v	velocity of light in medium
X	distance from final boundary of flow field to real Gaussian object plane
$x(t)$	distance from real Gaussian object plane to apparent Gaussian object plane
x,y	coordinates
$y(\alpha_w^*,t)$	displacement of light ray in final wind-tunnel window
y_i,η_i,μ_i	denotes value for given light ray at initial flow-boundary traversed by ray
y_i^*,η_i^*,μ_i^*	denotes value for given light ray at final flow-boundary traversed by ray
α	angle measured with respect to x coordinate
Δ	increment (Δy = distortion)
η	coordinate parallel to y coordinate
λ	wavelength of light
ν,σ	integers
μ	refractive index
ρ	density

Subscripts:

a	atmosphere
i	integer, refers to a given light ray

w	wind-tunnel window
δ	flow reference region (free stream)
ν, σ	integers

Superscripts:

*	refers to value at final flow-boundary traversed by light ray

2339

2339

APPENDIX B

LIGHT PATH IN FLOW FIELD

The light path in the flow field is obtained as the solution of the variation problem

$$\int dt = \frac{1}{c}\int \mu\sqrt{1 + \left(\frac{d\eta}{dx}\right)^2}\, dx = \text{stationary value} \tag{6}$$

where $\mu = \mu(y)$. Equation (6) is of the form

$$\int dt = \int F\left(\eta, \frac{d\eta}{dx}\right) dx \tag{B1}$$

the solution of which is given by the Euler equation

$$F - \eta' \frac{\partial F}{\partial \eta'} = \text{constant} \tag{B2}$$

where $\eta' = \frac{d\eta}{dx}$. Thus the solution of equation (6) is

$$1 + \left(\frac{d\eta}{dx}\right)^2 = \left(\frac{\mu}{\mu_i}\right)^2 \tag{7}$$

where $\mu = \mu_i$ at $y = y_i$. Let the light path be expressed by the Maclaurin series

$$\eta = \sum_{\sigma=0}^{\infty} c_\sigma x^\sigma \tag{11}$$

where the coefficients c_σ are given by

$$c_\sigma = \frac{1}{\sigma!}\left(\frac{d^\sigma \eta}{dx^\sigma}\right)_{\eta=0} \tag{B3}$$

It follows that

$$\frac{d\eta}{dx} = \sum_{\sigma=1}^{\infty} \sigma c_\sigma x^{\sigma-1} \tag{B4}$$

The assumed refractive index distribution

$$\mu = \sum_{\nu=0}^{\infty} b_\nu \eta^\nu \tag{9}$$

expression (B4), and finally series (11) are substituted in the differential equation (7) to obtain the expression

2339

$$1 + \left(\sum_{\sigma=1}^{\infty} \sigma c_\sigma x^{\sigma-1}\right)^2 = \left(\frac{1}{b_0}\right)^2 \left[b_0 + \sum_{\nu=1}^{\infty} \sum_{\sigma=0}^{\infty} b_\nu (c_\sigma x^\sigma)^\nu\right]^2 \tag{B5}$$

The right-hand side of equation (B5) may be replaced by its binomial expansion. However, only the first two terms of the three-term expansion need be retained because the coefficient b_0 represents the refractive index μ_i at $\eta = 0$. Since μ is very nearly unity over a wide range of temperatures and pressures, the third term of the binomial expansion is negligible. Therefore, equation (B5) becomes

$$\left(\sum_{\sigma=1}^{\infty} \sigma c_\sigma x^{\sigma-1}\right)^2 = 2 \sum_{\nu=1}^{\infty} \sum_{\sigma=0}^{\infty} b_\nu (c_\sigma x^\sigma)^\nu \tag{B6}$$

where $b_0 = 1$. When coefficients of like powers of x are equated, the coefficients c_σ may be expressed as functions of the refractive index coefficients b_ν. The first few coefficients c_σ are

$$\left.\begin{aligned}
c_0 &= c_1 = c_3 = c_5 = \ldots = c_{2\sigma-1} = 0 \\
c_2 &= \frac{1}{2} b_1 \\
c_4 &= \frac{1}{12} b_1 b_2 \\
c_6 &= \frac{1}{180} b_1 b_2^2 + \frac{1}{40} b_1^2 b_3 \\
c_8 &= \frac{1}{5040} b_1 b_2^3 + \frac{3}{560} b_1^2 b_2 b_3 + \frac{1}{112} b_1^3 b_4 \\
&\vdots \qquad\qquad \vdots
\end{aligned}\right\} \tag{12}$$

Replacing the coefficients c_σ in equation (11) by the corresponding expressions in terms of coefficients b_ν results in the following expression for the ray path:

$$\eta = \frac{1}{2} b_1 x^2 + \frac{1}{12} b_1 b_2 x^4 + \left(\frac{1}{180} b_1 b_2^2 + \frac{1}{40} b_1^2 b_3\right) x^6 +$$

2339

$$\left(\frac{1}{5040} b_1 b_2^3 + \frac{3}{560} b_1^2 b_2 b_3 + \frac{1}{112} b_1^3 b_4\right) x^8 + \ldots \qquad (13)$$

APPENDIX C

OPTICAL PATH RELATION

Given the fringe shift expression

$$S_i\lambda = (\mu_i-\mu_\delta)x^* + \frac{1}{\mu_i}\int_0^{x^*} \mu^2\,dx - \mu_i x^* + \mu_w\,(\overline{A_2A_3}-t) - \mu_a\,\overline{B_3B_5} \quad (20)$$

2339

the last two terms may be expressed by consideration of figure 2 as

$$\mu_w\,(\overline{A_2A_3}-t) = \mu_w t\left(\frac{1}{\cos\alpha_w^*} - 1\right) \quad (C1)$$

and

$$\mu_a\,\overline{B_3B_5} = -\,\mu_a\left[Kx^* - x(t) + t\right]\left(1 - \frac{1}{\cos\alpha_a^*}\right) \quad (C2)$$

respectively, where

$$X = Kx^* \quad (21)$$

The factors α_w^* and α_a^* in equations (C1) and (C2), respectively, may be expressed in terms of α^* by virture of Snell's law of optical refraction; that is,

$$\mu_i^*\sin\alpha^* = \mu_w\sin\alpha_w^* = \mu_a\sin\alpha_a^* \quad (C3)$$

and $x(t)$ may be replaced by

$$x(t) = t\left(1 - \frac{\mu_a}{\mu_w}\right) \quad (16)$$

Then equations (C1) and (C2) become, respectively,

$$\mu_w\,(\overline{A_2A_3}-t) = \mu_w t\left(\frac{1}{\sqrt{1 - \left(\frac{\mu_i^*}{\mu_w}\right)^2\sin^2\alpha^*}}\right) - 1 \quad (C4)$$

and

$$\mu_a \overline{B_3B_5} = - \mu_a \left(Kx^* + \frac{\mu_a}{\mu_w} t\right)\left(1 - \frac{1}{\sqrt{1 - \left(\frac{\mu_i^*}{\mu_a}\right)^2 \sin^2 \alpha^*}}\right) \tag{C5}$$

2339

Then, when $(1-\cos^2 \alpha^*)$ is substituted for $\sin^2 \alpha^*$ and $\cos \alpha^*$ is replaced by expression (15), that is,

$$\cos \alpha^* = \frac{\mu_i}{\mu_i^*}$$

equations (C4) and (C5) may be rewritten in the form

$$\mu_w \left(\overline{A_2A_3}-t\right) = \mu_w t \left(\frac{\mu_w}{\sqrt{\mu_w^2 + \mu_i^2 - \mu_i^{*2}}} - 1\right) \tag{C6}$$

and

$$\mu_a \overline{B_3B_5} = - \mu_a \left(Kx^* + \frac{\mu_a}{\mu_w} t\right)\left(1 - \frac{\mu_a}{\sqrt{\mu_a^2 + \mu_i^2 - \mu_i^{*2}}}\right) \tag{C7}$$

respectively. Substituting equations (C6) and (C7) in equation (20) and collecting terms yield

$$S_i\lambda = (\mu_i-\mu_\delta)\, x^* + \frac{1}{\mu_i}\int_0^{x^*} \mu^2\, dx - \mu_i x^* + \mu_a K x^* \left[\frac{\sqrt{\mu_a^2 + \mu_i^2 - \mu_i^{*2}} - \mu_a}{\sqrt{\mu_a^2 + \mu_i^2 - \mu_i^{*2}}}\right] +$$

$$t\left[\mu_w\left(\frac{\mu_w - \sqrt{\mu_w^2 + \mu_i^2 - \mu_i^{*2}}}{\sqrt{\mu_w^2 + \mu_i^2 - \mu_i^{*2}}}\right) + \frac{\mu_a^2}{\mu_w}\left(\frac{\sqrt{\mu_a^2 + \mu_i^2 - \mu_i^{*2}} - \mu_a}{\sqrt{\mu_a^2 + \mu_i^2 - \mu_i^{*2}}}\right)\right] \tag{22}$$

The right-hand side of expression (22) consists of a sequence of terms comprising differences of quantities of nearly equal value. Those terms which are included as roots may be expanded by means of the binomial theorem. Thus

$$\left.\begin{aligned}\sqrt{\mu_a^2 + \mu_i^2 - \mu_i^{*2}} &= \sum_{\nu=0}^{\infty} B_\nu \mu_a^{(1-2\nu)} \left(\mu_i^2 - \mu_i^{*2}\right)^\nu \\ \sqrt{\mu_w^2 + \mu_i^2 - \mu_i^{*2}} &= \sum_{\nu=0}^{\infty} B_\nu \mu_w^{(1-2\nu)} \left(\mu_i^2 - \mu_i^{*2}\right)^\nu\end{aligned}\right\} \tag{C8}$$

2339

where the binomial coefficients B_ν are $B_0 = 1$, $B_1 = \frac{1}{2}$, $B_2 = -\frac{1}{8}$, $B_3 = \frac{1}{16}$, . . . The series (C8) converge because $\mu_w^2 > \mu_a^2 >> \mu_i^{*2} - \mu_i^2$. Moreover, because for $\nu > 1$ the terms of expansions (C8) comprise products of differences of quantities of nearly equal value, such terms may be regarded as negligible. Hence expression (22) may be reduced to

$$S_i\lambda = (\mu_i - \mu_\delta)x^* + \frac{1}{\mu_i}\int_0^{x^*} \mu^2\, dx - \mu_i x^* - \frac{1}{2} Kx^*\left(\mu_i^{*2} - \mu_i^2\right) \tag{C9}$$

where $\mu_a \approx 1$ except when differences of quantities of nearly equal value are concerned. Furthermore, because $\mu_i \approx \mu_i^*$

$$\mu_i^{*2} - \mu_i^2 \approx 2\mu_i(\mu_i^* - \mu_i) \tag{C10}$$

so that approximation (C9) may be rewritten as

$$S_i\lambda = (\mu_i - \mu_\delta)x^* + \frac{1}{\mu_i}\int_0^{x^*} \mu^2\, dx - \mu_i x^* - Kx^*(\mu_i^* - \mu_i) \tag{23}$$

Substituting expansion (9) in (23) and replacing η by series (11), both expansions being assumed convergent, yield the following expression for approximation (23):

$$S_i\lambda = (\mu_i - \mu_\delta)x^* + \frac{1}{\mu_i}\int_0^{x^*} \left[\mu_i^2 + 2\mu_i \sum_{\nu=1}^{\infty} b_\nu \left(\sum_{\sigma=2,4,6,\ldots}^{\infty} c_\sigma x^\sigma\right)^\nu\right] dx -$$

$$\mu_i x^* - \mu_i\, Kx^* \sum_{\nu=1}^{\infty} b_\nu \left(\sum_{\sigma=2,4,6,\ldots}^{\infty} c_\sigma x^{*\sigma}\right)^\nu \tag{C11}$$

where the third term of the binomial expansion of μ^2 is negligible. Equation (C11) may be rewritten in the form

$$S_i\lambda = (\mu_i-\mu_\delta)x^* + \frac{1}{\mu_i}\int_0^{x^*}\left[\mu_i^{\,2} + 2\mu_i\sum_{\nu=1}^{\infty}\sum_{\sigma=2,4,6,\ldots}^{\infty} b_\nu c_{\sigma\nu}x^\sigma\right]dx -$$

2339

$$\mu_i x^* - \mu_i\, Kx^*\sum_{\nu=1}^{\infty}\sum_{\sigma=2,4,6,\ldots}^{\infty} b_\nu c_{\sigma\nu}x^{*\sigma} \tag{C12}$$

where the coefficients $c_{\sigma\nu}$ are expressed in terms of the coefficients c_σ by equating the coefficients of like powers of x in the expression

$$\sum_{\sigma=2,4,6,\ldots}^{\infty} c_{\sigma\nu}x^\sigma = \left(\sum_{\sigma=2,4,6,\ldots}^{\infty} c_\sigma x^\sigma\right)^\nu \tag{25}$$

Integrating equation (C12) and solving for $\mu_i - \mu_\delta$ result in

$$\mu_i - \mu_\delta = S_i\,\frac{\lambda}{x^*} - 2\sum_{\nu=1}^{\infty}\sum_{\sigma=2,4,6,\ldots}^{\infty}\frac{b_\nu c_{\sigma\nu}}{\sigma+1}\,x^{*\sigma} + K\sum_{\nu=1}^{\infty}\sum_{\sigma=2,4,6,\ldots}^{\infty} b_\nu c_{\sigma\nu}x^{*\sigma} \tag{24}$$

where the multiplicative constant μ_i in the last sum of equation (C12) is regarded as unity.

APPENDIX D

OPTICAL DISTORTION

From equation (27), that is,

$$(\Delta y)_i = \left[Kx^* - x(t) + t\right] \tan \alpha_a^* - \left[\eta_i^* + y(\alpha_w^*, t)\right] \tag{27}$$

it follows by virtue of Snell's law (equation (C3)) and equation (15) that 2339

$$\sin \alpha_a^* = \frac{1}{\mu_a} \sqrt{\mu_i^{*2} - \mu_i^2}$$

$$\cos \alpha_a^* = \frac{1}{\mu_a} \sqrt{\mu_a^2 + \mu_i^2 - \mu_i^{*2}} \tag{D1}$$

$$\tan \alpha_a^* = \sqrt{\frac{\mu_i^{*2} - \mu_i^2}{\mu_a^2 + \mu_i^2 - \mu_i^{*2}}}$$

Also,

$$y(\alpha_w^*, t) = t \tan \alpha_w^* = \frac{\mu_a}{\mu_w} t \frac{\sin \alpha_a^*}{\sqrt{1 - \left(\frac{\mu_a}{\mu_w}\right)^2 \sin^2 \alpha_a^*}} \tag{D2}$$

Then, because of equations (D1),

$$y(\alpha_w^*, t) = t\sqrt{\frac{\mu_i^{*2} - \mu_i^2}{\mu_w^2 + \mu_i^2 - \mu_i^{*2}}} \tag{D3}$$

When $x(t)$ is replaced by expression (16) and equations (D1) and (D3) are utilized, equation (27) becomes

$$(\Delta y)_i = \left(Kx^* + \frac{\mu_a}{\mu_w} t\right)\sqrt{\frac{\mu_i^{*2} - \mu_i^2}{\mu_a^2 + \mu_i^2 - \mu_i^{*2}}} - \left(\eta_i^* + t\sqrt{\frac{\mu_i^{*2} - \mu_i^2}{\mu_w^2 + \mu_i^2 - \mu_i^{*2}}}\right) \tag{28}$$

Assuming that $\mu_i \approx \mu_i^* \approx \mu_a \approx 1$, except where differences of quantities of nearly equal value comprise a complete term, equation (28) reduces to

$$(\Delta y)_i = Kx^* \sqrt{\mu_i^{*2} - \mu_i^2} - \eta_i^* \tag{29}$$

2339

Rather than expand the square root term of approximation (29) by the binomial expansion, which converges very slowly because $\mu_i^* \approx \mu_i$, the term may be replaced by $\left(\frac{d\eta}{dx}\right)_{\eta=\eta_i^*}$, where $\mu_i \approx 1$, which follows from equation (7) so that

$$(\Delta y)_i = Kx^* \left(\frac{d\eta}{dx}\right)_{\eta=\eta_i^*} - \eta_i^* \tag{30}$$

Finally, because of series (11) and its derivative, series (B4),

$$(\Delta y)_i = \sum_{\sigma=2,4,6,\ldots}^{\infty} (K\sigma - 1)\, c_\sigma x^{*\sigma} \tag{31}$$

REFERENCES

1. Schardin, Hubert: Toepler's Schlieren Method, Basic Principles for Its Use and Quantitative Evaluation. Trans. 156, The David W. Taylor Model Basin, Navy Dept., July 1947.

2. Jenkins, Francis A., and White, Harvey E: Fundamentals of Physical Optics. McGraw-Hill Book Co., Inc. (New York), 1937, pp. 1-104.

3. Eckert, Ernst R. G., Drake, R. M., Jr., and Soehngen, Eric: Manufacture of a Zehnder-Mach Interferometer. Tech. Rep. 5721, Air Materiel Command (Wright-Patterson Air Force Base), Aug. 31, 1948.

4. Bershader, Daniel: An Interferometric Study of Supersonic Channel Flow. Rev. Sci. Instruments, vol. 20, no. 4, April 1949, pp. 260-275.

5. Wachtell, G. P.: Refraction Effect in Interferometry of Boundary Layer of Supersonic Flow Along Flat Plate. Appendix to: Progress Rep. No. 19, The Study of Supersonic Flow by Interferometry and Other Optical Methods by R. Ladenburg. Palmer Physical Laboratory, Princeton Univ., Dec. 19, 1949. (Contract N7 ONR 399, Task Order 1.)

6. Blue, Robert E.: Interferometer Corrections and Measurements of Laminar Boundary Layers in Supersonic Stream. NACA TN 2110, 1950.

7. Bromwich, T. J. I'a.: An Introduction to the Theory of Infinite Series. Macmillan and Co., Ltd. (London), 1942, pp. 317-393.

8. Kingslake, R.: The Interferometer Patterns Due to the Primary Aberrations. Trans. Optical Soc. (London), vol. 27, no. 2, 1925-1926, pp. 94-105.

2339

2339

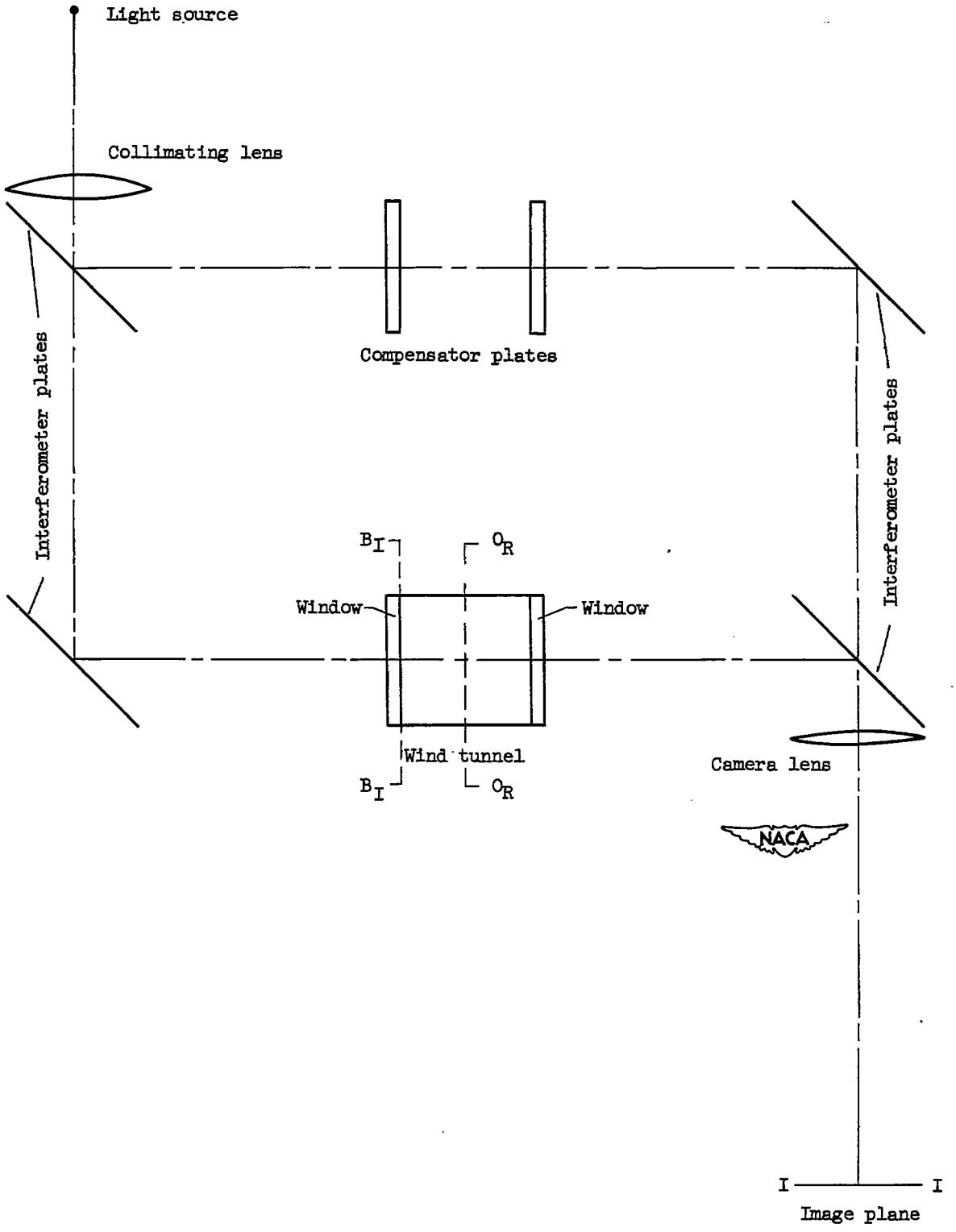

Figure 1. - Interferometer apparatus.

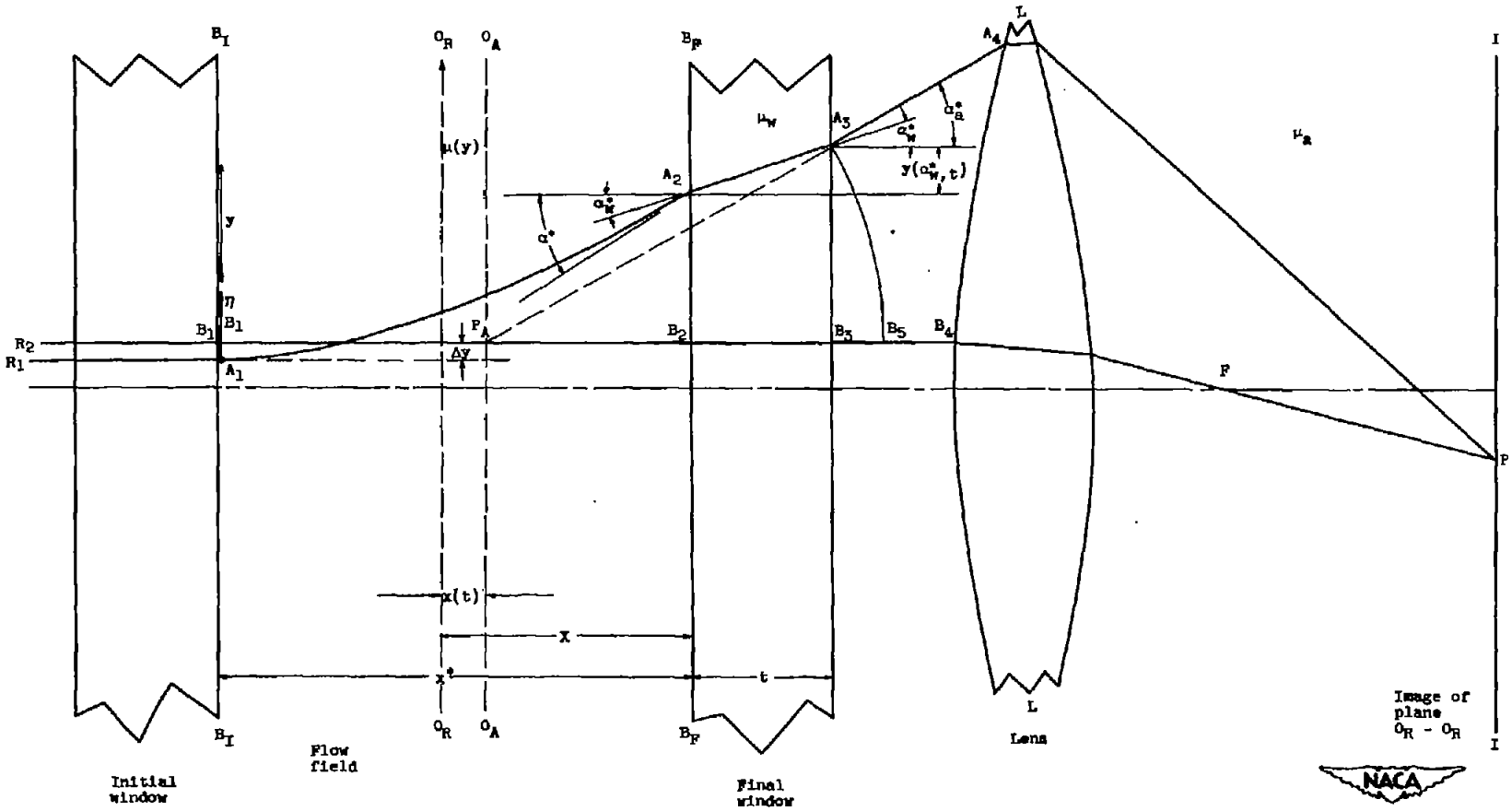

Figure 2. - Light path detail. Ray R_1 traverses wind tunnel; ray R_2 circumvents wind tunnel.

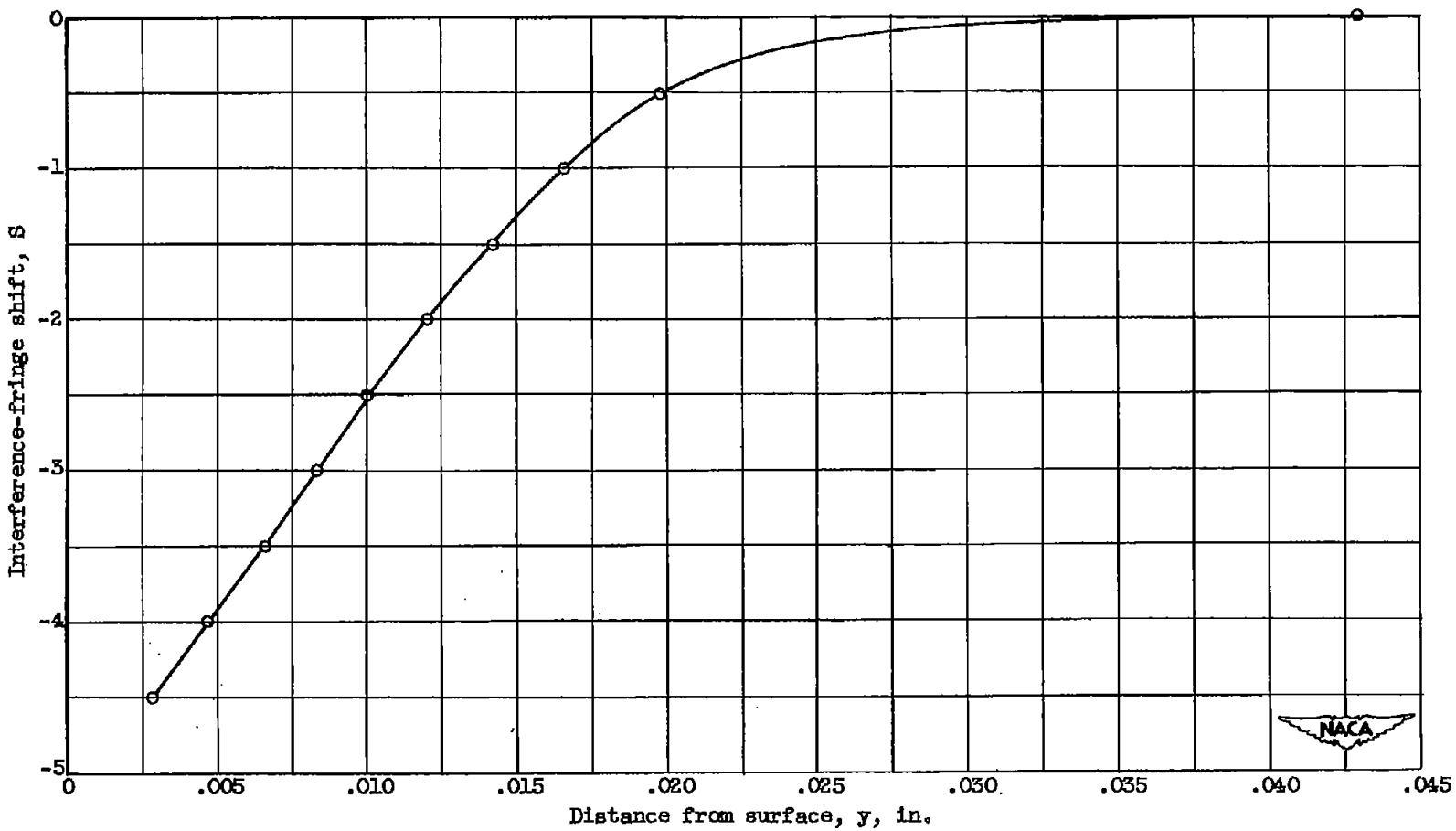

Figure 3. - Variation of interference-fringe shift with distance from surface of flat plate. Fraction of wind tunnel span, K, 0.5.

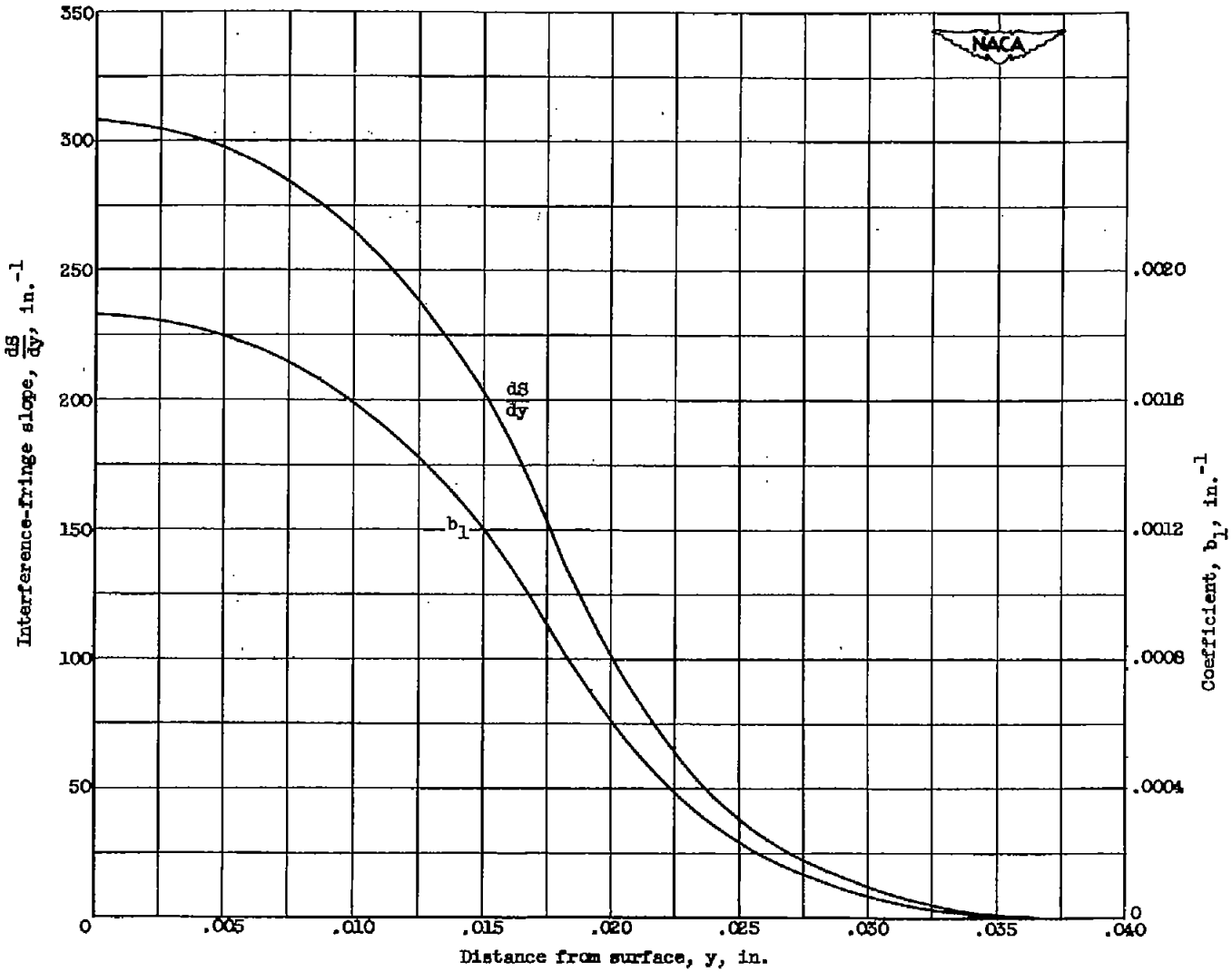

Figure 4. - Variation of interference-fringe slope and coefficient b_1 with distance from surface of flat plate. Fraction of wind tunnel span, K, 0.5.

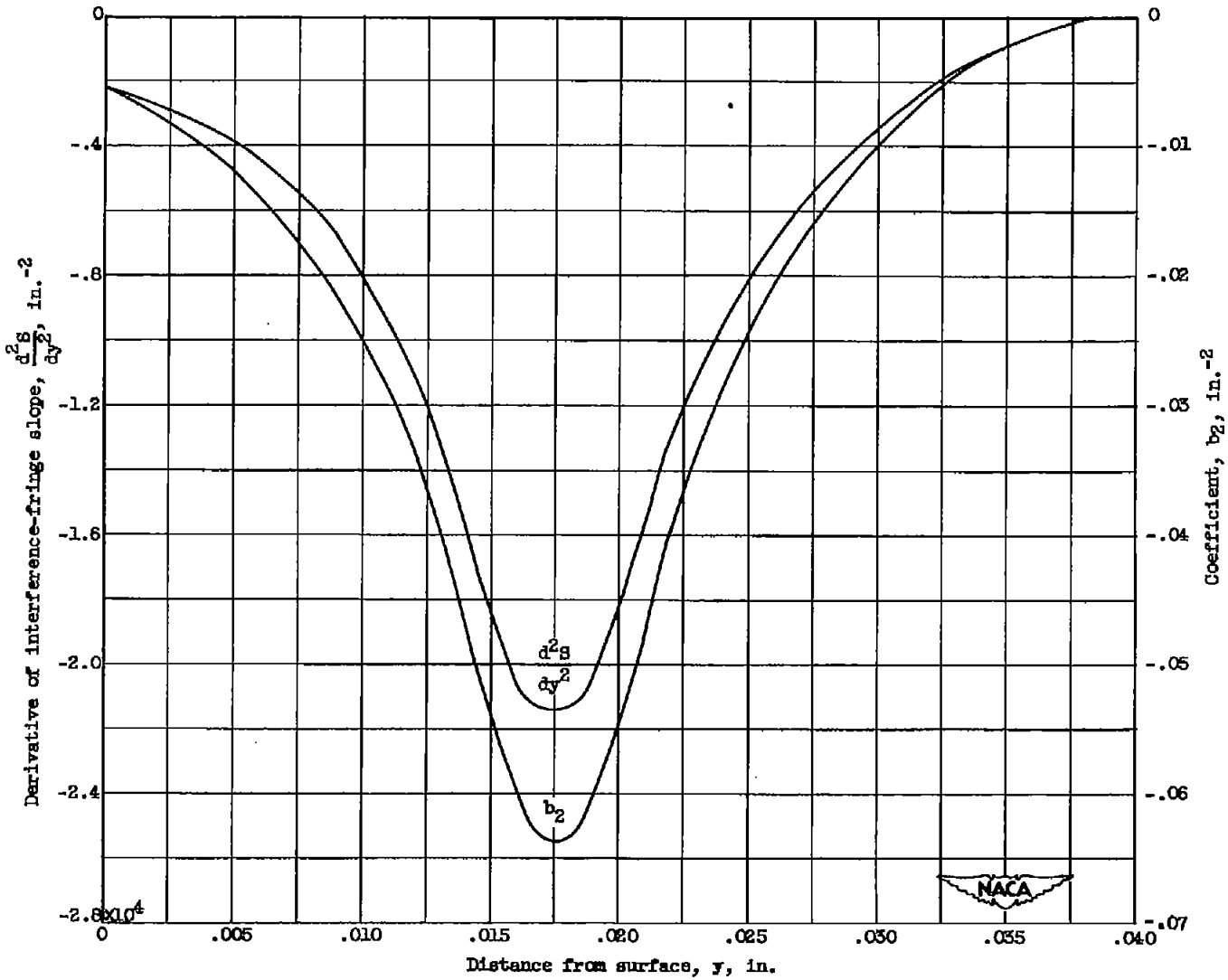

Figure 5. - Variation of derivative of interference-fringe slope and coefficient b_2 with distance from surface of flat plate. Fraction of wind tunnel span, K, 0.5.

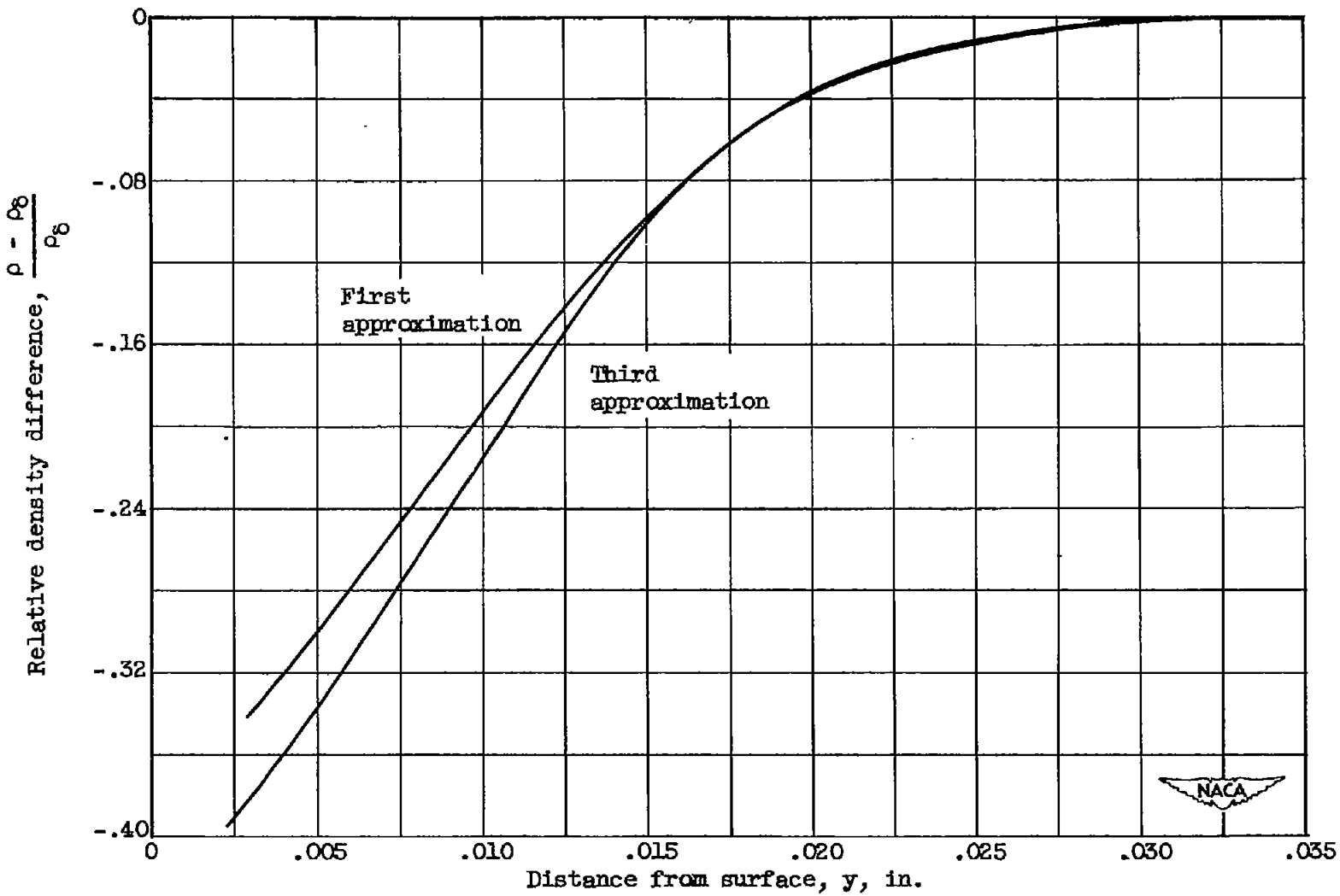

Figure 6. - Density profiles indicated by interference measurements.

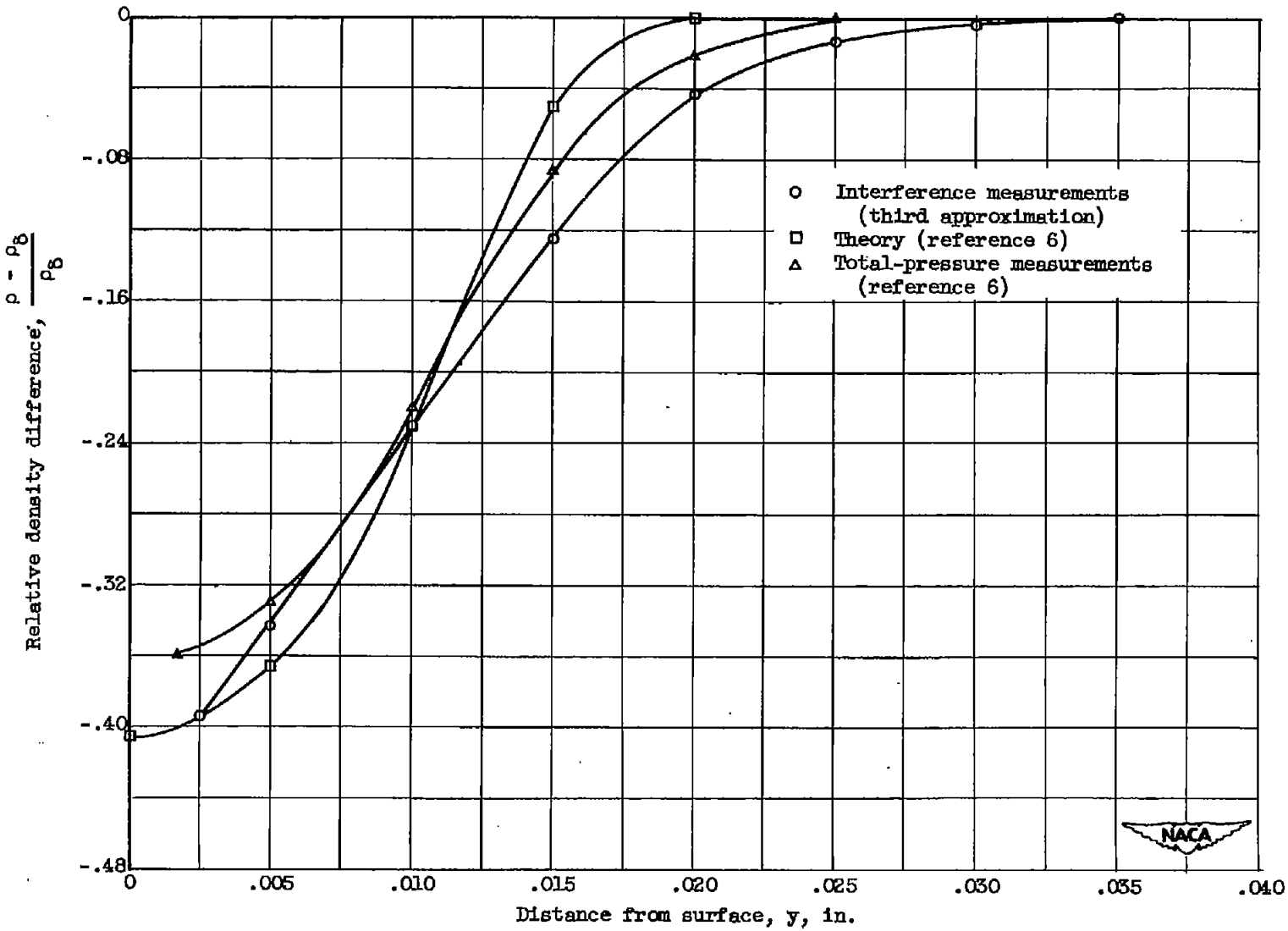

Figure 7. - Comparison of density profiles indicated by various methods.

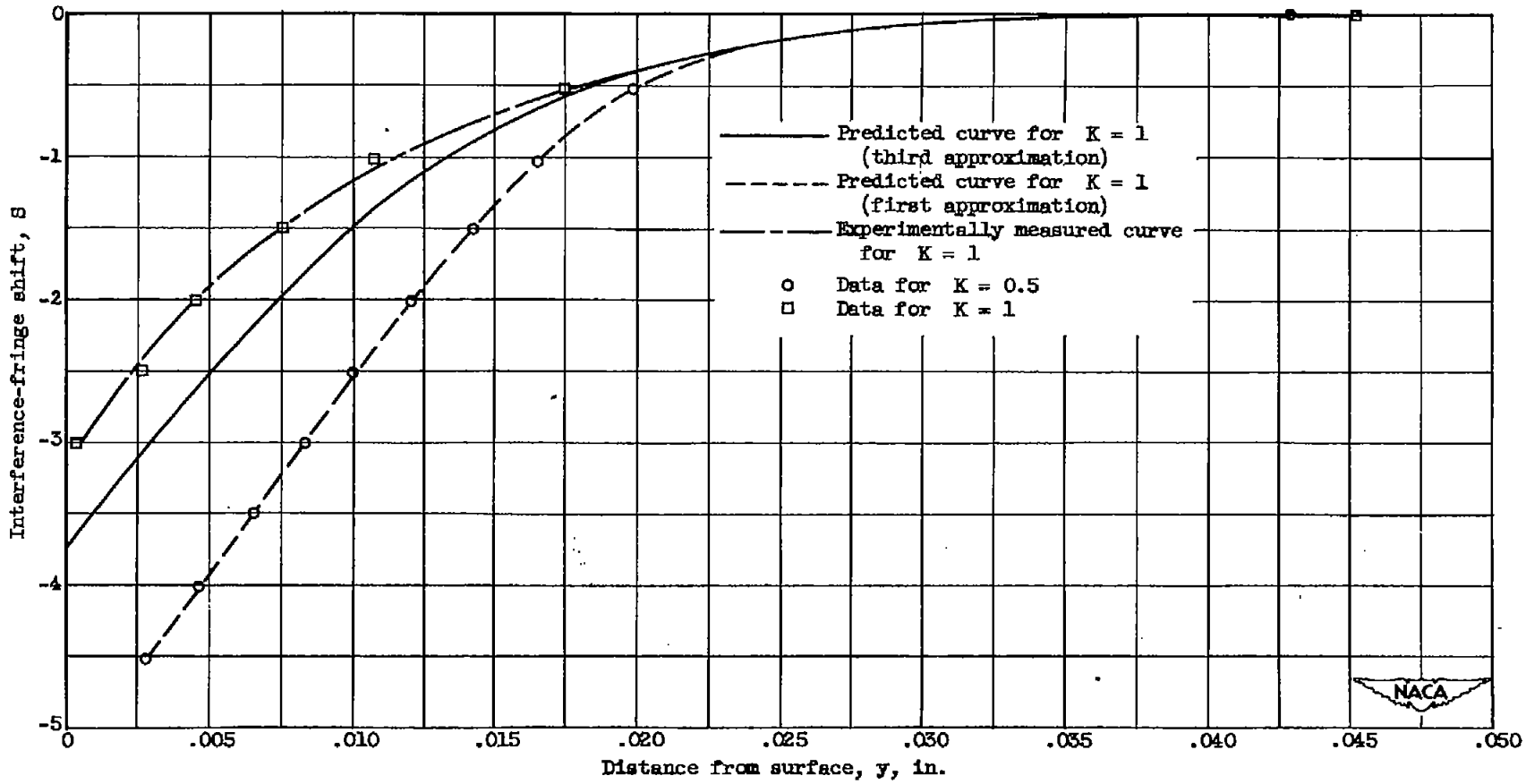

Figure 8. - Predicted curve of fringe shift for fraction of wind tunnel span K = 1 from data for K = 0.5.

NACA-Langley - 4-23-52 - 1000